tvst

Article

The Existence and Regression of Persistent Bergmeister's Papilla in Myopic Children Are Associated With Axial Length

Qiurong Lin[1,2,*], Junjie Deng[1,2,*], Kyoko Ohno-Matsui[3], Xiangui He[2], and Xian Xu[1,2]

[1] Shanghai Eye Diseases Prevention & Treatment Center, Shanghai Eye Hospital, Shanghai, China
[2] Shanghai General Hospital, Shanghai Jiao Tong University School of Medicine, Shanghai, China
[3] Department of Ophthalmology and Visual Science, Tokyo Medical and Dental University, Bunkyo-ku, Tokyo, Japan

Correspondence: Xian Xu, Shanghai General Hospital, Shanghai Jiao Tong University School of Medicine, Shanghai, No. 100 Haining Road, Shanghai, People's Republic of China 200080, China.
e-mail: drxuxian@163.com

Received: May 14, 2021
Accepted: October 4, 2021
Published: November 2, 2021

Keywords: axial length (AL); myopia; optic disc; Bergmeister's papilla

Citation: Lin Q, Deng J, Ohno-Matsui K, He X, Xu X. The existence and regression of persistent Bergmeister's papilla in myopic children are associated with axial length. Transl Vis Sci Technol. 2021;10(13):4, https://doi.org/10.1167/tvst.10.13.4

Purpose: The purpose of this study was to evaluate the existence and regression of persistent Bergmeister's papilla (PBP) in myopic eyes and determine its independent predictors.

Methods: This cross-sectional population-based study included 472 eyes of 236 myopic children. PBPs were identified with swept-source optical coherence tomography (OCT) and were classified into three types (types I, II, and III) according to their morphologic features.

Results: The mean patient age was 12.13 ± 2.60 years (range = 5–18 years), and 118 (50%) participants were boys. The prevalence of PBPs in our study was 67.8% (160/236). There were significant differences in height, spherical equivalent (SE), and axial length (AL) between the PBP and non-PBP groups ($P < 0.05$). Type I PBP was noted in 173 eyes (66.8%); type II PBP in 59 eyes (22.8%); and type III PBP in 27 eyes (10.4%). The three PBP types showed significant differences in height, AL, and SE ($P < 0.001$). Stepwise linear regression analysis indicated that the height (B = 4.497, $P < 0.001$), PBP existence or not (B = −1.434, $P < 0.001$), and the types of PBP (B = 0.566, $P = 0.041$) was an independent predictor for AL, respectively. PBP was detected more frequently in the nasal quadrant than in the inferior quadrant of the disc.

Conclusions: PBP regression was closely related to the AL and could be used as a new biomarker to indicate the progression of myopia.

Translational Relevance: Our analysis of the presence and morphology of PBP might enable clinicians to judge the progression of myopia.

Introduction

The hyaloid remnants on the optic disc are vestiges of the narrow sheath closely surrounding the hyaloid vessel during embryonic life. In 1877, Bergmeister described a cone-shaped collection of cells in the central excavation of the disc as the primitive epithelial papilla, and subsequently, a grey mass in that region was referred to as the Bergmeister papilla. The hyaloid artery atrophies during embryonic life or at the beginning of postembryonic life. The Bergmeister papilla can also show regression when atrophy is not complete, leaving a large amount of colloid tissue on the optic disc; the common histologic findings in such cases include a vascular component, glial cells, and connective tissue, which are referred to as persistent Bergmeister's papilla (PBP).[1]

Few studies have assessed PBPs to date. In 1963, Jones et al.[2] observed 100 premature infants (maturity = 26–38 weeks) by using traditional ophthalmoscopy after pupil dilation and found that 95% of the infants had transparent residues in front of the optic disc of one or both eyes at 1 to 2 weeks after birth; similar examinations in a control series of mature infants (n = 100) revealed hyaloid remnants in only 3%. In 1972, Roth et al.[3] used a stereomicroscope and a separate high-intensity illuminator to observe cadaver eyes fixed in 10% formalin (n = 504; age range = from birth to 88 years) and found that PBP was seen in 162 (32.14%)

eyes. Recently, Bassi et al.[4] reported that the prevalence of PBP was 0.03% in an adult population (age ≥40 years, $n = 6013$) by using a fundus camera (one stereo pair of 20 degrees optic disc photographs). In 2014, Liu et al.[5] detected PBPs in 11 eyes (50%) of 22 healthy subjects (mean age = 33.0 years, range = 23–49 years) by using swept-source optical coherence tomography (SS-OCT), which was much higher than the prevalence observed by conventional ophthalmoscopy or fundography. Liu et al.[5] believed that this may be because OCT offers improved visualization of the PBP. OCT is a novel modality that allows noninvasive, volumetric, and measurable in vivo visualization of the anatomic microstructural features of the posterior vitreous and vitreoretinal interface. The development of SS-OCT technology has enabled higher speeds, better sensitivity with imaging depth, and longer imaging range, thereby allowing better visualization of the vitreoretinal interface and posterior vitreous cortex, even on the optic disc.[5]

In addition to the differences in the resolutions afforded by the techniques and instruments, another reason for the large discrepancies in the prevalence of PBPs in the previous studies include differences in the age, eye development, and other individual factors of the subjects. Jones et al.[2] followed up 26 premature infants over 9.69 ± 3.90 weeks (range = 2–20 weeks) and found that the hyaloid remnants gradually disappeared, passing through the stages of filament, filament with broad base, collapsed sail, and a dot. Therefore, we speculate that PBPs in full-term children may be gradually absorbed after birth during the growth and development of the eyeball. During the process of absorption, PBPs can present in a variety of forms, reflecting the different stages of the absorption process. However, does the existence and absorption of PBPs have a characteristic clinical significance in eye diseases (i.e. myopia), which threatens the healthy development of children and adolescents' eyes?[6] Myopia (defined by spherical equivalent [SE] ≤ −0.5 diopters [D]) now is a widespread condition, typically starts in childhood, and is reaching epidemic proportions, especially in east Asia, with the prevalence of myopia in young adults (at the age of 17–18 years) around 80% to 90%, and an accompanying high prevalence of high myopia (10–20%).[7] Early detection or prevention is the main public health strategy to limit myopia progression. At present, no study in children has attempted a relative assessment of the different features of PBPs or evaluated the relationship between PBP features and eye indexes, such as axial length (AL).

To explore the significance of PBPs absorption and morphology in the eyes of myopic children, the present series of investigations were undertaken. This preliminary cross-sectional study was based on the SS-OCT findings in a relatively large sample of myopic children. We aimed to determine the prevalence of PBPs and their relationship with age, gender, refractive error, and different features and distribution of PBPs.

Methods

This cross-sectional population-based study was conducted at the Shanghai First People's Hospital and Shanghai Eye Disease Prevention and Treatment Center. The project was approved by the Ethics Committee of Shanghai General Hospital, Shanghai Jiao Tong University (2018KY209). It was carried out in accordance with the Declaration of Helsinki. Written informed consent was obtained from the legal guardian of each child at the examination site.

Study participants were children who were recruited during the Shanghai Child and Adolescent Large-scale Eye Study-High Myopia Registration from August 2018 through September 2018. The inclusion criteria were as follows: (1) both eyes were diagnosed as myopia, an SE was −0.50 D or less; (2) no systemic disease; (3) full-term birth with good growth and development; and (4) best corrected visual acuity (BCVA) of both eyes ≥0.8. The exclusion criteria were as follows: (1) both eyes showed the presence of eye diseases other than refractive error, such as macular edema, optic neuropathy, and hereditary eye diseases; (2) inability to cooperate with the examination and poor image quality; and (3) the presence of systemic diseases, such as hypertension, respiratory system diseases, circulatory system diseases, diabetic mellitus, or urinary system diseases.

Using the formula $N = (Z)^2\ (1.0 - P)(P)/[(B)(P)]^2$, the sample size was based on estimation of an anticipated 50% prevalence of PBPs as observed by SS-OCT in healthy subjects within an error bound (precision) of 20% with 95% confidence.[5] A sample of 96 children was required.

The participants' personal information was collected using a detailed questionnaire that included questions regarding age, gender, date of birth, family history of disease, years of education, general medical history, eye disease history, and history of eye surgery. The patients' height and weight (Model EF07; Hochoise, Shanghai, China) were measured by the general health practitioners. Body mass index (BMI) was calculated as the patients' weight (Kg) divided by their height squared (m^2). All patients underwent a complete ophthalmological examination, including assessment of BCVA and the refractive power after

cycloplegic autorefraction using an autorefractor (KR-8900; Topcon Medical Systems, Tokyo, Japan), measurement of the AL and lens thickness (LT) with IOL Master 900 (Carl Zeiss Meditec, Dublin, CA, USA), intraocular pressure (IOP) measurement with a noncontact tonometer (NT510; NIDEK, Tokyo, Japan), examination of the eyelid, globe, pupillary reflex, and lens, and silt lamp biomicroscopy (YZ5 × 1; 66 Vision-Tech Co., Ltd, Suzhou, China) of the fundus with spherical +90 D lenses (Volk, Mentor, OH, USA) after pupil dilation. Fundus photographs centered at the optic disc and macula were taken with the Topcon TRC 50DX Retinal Camera (Topcon Medical Systems).

SS-OCT (DRI OCT-1; Topcon Medical Systems) was acquired using 12 radial meridian scans with a diameter of 9 mm centered on the optic disc. The length of the maximum section of the PBP (the distance from the center point of the optic disc surface to the vertex in the vitreous cavity) and the width of the base (the distance between the two end points on the optic disc surface) were measured by using the built-in measuring tool, and the ratio of these values (length/base width) was calculated.

On the basis of the morphologic features, we divided PBPs into three types: type I, type II, and type III. All three types showed the presence of an obvious base attached to the optic disc and a body lying in the vitreous in at least one OCT scan, with the body protruding above the nerve fibers, with or without a signal attenuation/shadow behind the base (dark area) or the retinal blood vessels below (dark area). In type I PBP, on one

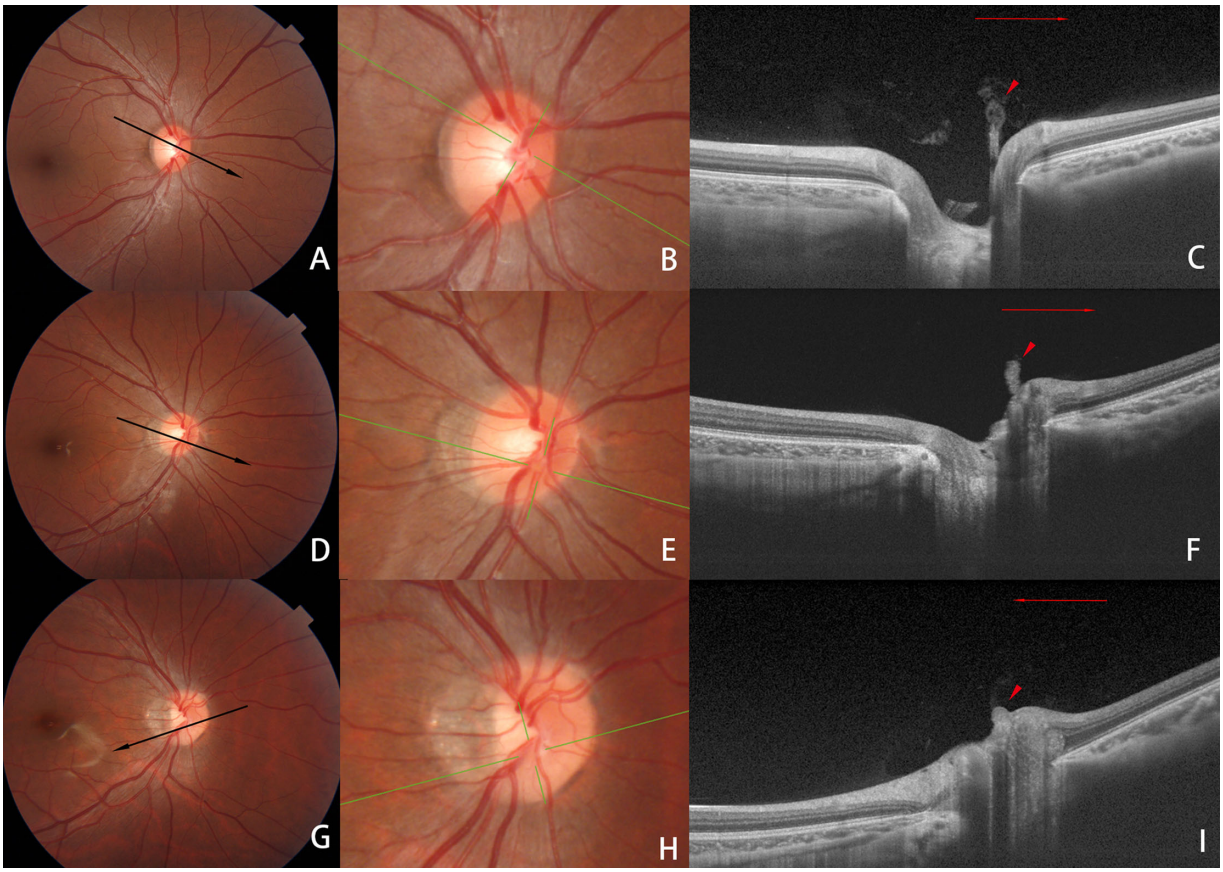

Figure 1. Fundus photographs and swept-source OCT images of eyes with PBPs. (**A**) Fundus photograph of the right eye of a 9-year-old boy showing PBP nasal to the optic disc. The refractive error was −2.0 D, and the AL was 23.58 mm. Black line is the OCT scan line. (**B**) Magnified images of **A**. (**C**) B-scan swept-source OCT image of the scanned line shown in **A** showing type I PBP (arrowheads), the boundary of the distal end of the body was not clearly defined, diffuse, and appeared like a flame, with a signal attenuation/shadow behind the base. (**D**) Right fundus photograph of a 13-year-old boy showing PBP nasal to the optic disc. The refractive error was −5.4 D, and the AL was 25.53 mm. (**E**) Magnified images of **D**. (**F**) B-scan swept-source OCT image showing type II PBP (arrowheads), the boundary of the distal end of the body was obtuse and dense with length/base width >1. (**G**) Right fundus photograph of a 16-year-old boy showing PBP inferior to the optic disc. The refractive error was −7.5 D and the AL was 27.00 mm. Black line is the OCT scan line. (**H**) Magnified images of **G**. (**I**) B-scan swept-source OCT image along the scanned line showing type III PBP (arrowheads), the boundary of the distal end of the body was obtuse and dense with length/base width ≤1.

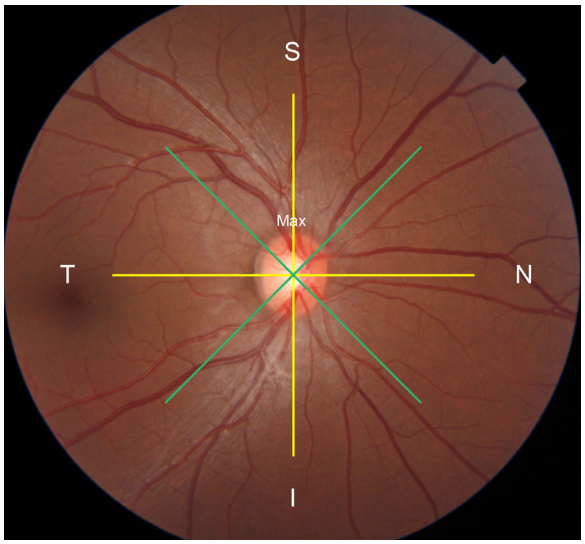

Figure 2. Schematic diagram of optic disc partition. The maximum axis and the minimal axis (yellow lines) of the optic disc were defined as the vertical meridian and the horizontal meridian, separately. Two oblique lines (green lines) divided the optic disc into superior, inferior, nasal, and temporal quadrants.

OCT scan image, the boundary of the distal end of the body (the portion extending to the vitreous, far away from the optic disc) was not clearly defined, diffuse, and appeared like a flame. In type II PBP, on any OCT scan, the boundary of the distal end of the body was obtuse and dense. One or more OCT scans will show body length/base width >1, similar to a cylindrical or conical shape. In type III PBP, on any OCT scan, the boundary of the distal end of the body was obtuse and dense. Each OCT scan will show body length/base width ≤1, similar to a hillock shape (Fig. 1).

Children who showed PBPs in the observed region of either eye were categorized into the PBP group. We divided the optic disc into superior, inferior, nasal, and temporal quadrants. Then, we chose the middle point of the PBP base to determine its position.

The major (maximum) axis of the optic disc was defined as the vertical meridian, and the minimal axis as the horizontal meridian (Fig. 2).

Statistical Analyses

Statistical analyses were performed with the SPSS version 24.0 software (IBM, Armonk, NY, USA). The BCVA was measured with a Snellen chart, and the decimal acuities were converted to logarithm of the minimum angle of resolution (logMAR) values for statistical analysis. Continuous data were presented as mean ± standard deviation (SD) values, and categorical data were presented as frequency and percentage. For continuous variables, the independent Student *t*-test was used if the values followed a normal distribution; if not, the Mann–Whitney *U* test was performed to compare the differences in various values between the PBP and non-PBP groups. The categorical variables were compared using the chi-squared test. One-way ANOVA analysis and Kruskal–Wallis test were used to explore the factors influencing the three types of PBPs. Then, linear regression analysis was performed using the "stepwise" method, and independent variables with PBP existence or not, types of PBP, length/base width, sex, age, height, weight, BMI, IOP, LT, and BCVA (logMAR) were included to identify the independent influencing factors for the AL.

Results

A total of 236 children aged ≤18 years were included, meeting the sample size requirements. Overall, 118 (50%) children were boys. The mean age ± SD of the participants was 12.13 ± 2.60 years; the mean height ± SD was 1.57 ± 0.15 m; mean weight ± SD was 48.89 ± 15.68 kg; and mean BMI ± SD was 19.44 ± 3.75 kg/m^2.

There was no significant difference in AL, SE, LT, IOP, and BCVA (logMAR) between the left and right eyes (Table 1). Therefore, we used binocular mean SE, binocular mean LT, binocular mean IOP, binocular mean AL, and binocular mean BCVA (logMAR) for statistical analysis of the correlation factors.

Among the 236 children, 160 (67.80%) showed PBPs, and the remaining 76 (32.2%) did not show PBPs (Table 2). According to univariate analysis, there were no statistically significant intergroup differences in gender, age, weight, BMI, binocular mean LT, and IOP. Participants in the PBP group were more likely to be shorter ($P = 0.027$), less likely to be myopic ($P = 0.003$), and had shorter AL ($P = 0.003$).

A total of 259 eyes of 160 children with PBPs were studied. PBPs were observed bilaterally in 98 children and unilaterally in the other 62 children. On the basis of OCT findings, type I PBP was observed in 173 eyes (66.8%); type II PBP in 59 eyes (22.8%); and type III PBP in 27 eyes (10.4%). From type I through type III, the shape of the PBP gradually changed from a slender shape extending in the vitreous cavity (similar to the hyaloid artery) to a flat shape gathering in front of the optic disc.

The differences in AL, SE, LT, IOP, and BCVA among the three types of PBP eyes were analyzed (Table 3). We found that a higher AL or degree of myopia corresponded to a greater incidence of type III

Table 1. Consistency Test of Left and Right Eye Parameters

	Left Eye	Right Eye	*P* Value
Axial length, mm	25.69 ± 1.40	25.94 ± 1.22	0.063
Spherical equivalent, D	−5.68 ± 2.57	−5.99 ± 2.50	0.184
Lens thickness, mm	3.35 ± 0.17	3.36 ± 0.16	0.253
Intraocular pressure, mm Hg	15.61 ± 2.73	15.59 ± 2.72	0.953
BCVA (logMAR)	−0.01 ± 0.03	−0.01 ± 0.02	0.853

P, paired *t*-test; BCVA, best corrected visual acuity; logMAR, logarithm of the minimum angle of resolution.

Table 2. Demographic and Clinical Characteristics

	PBP Group ($n = 160$)	Non-PBP Group ($n = 76$)	*P* Value
Male	74	44	0.095
Female	86	32	
Age, y	12.05 ± 2.66	12.30 ± 2.49	0.487
Height, m	1.55 ± 0.16	1.60 ± 0.14	0.027
Weight, kg	48.02 ± 16.08	50.74 ± 14.74	0.213
Body mass index (kg/m^2)	19.42 ± 3.96	19.48 ± 3.28	0.910
Binocular mean spherical equivalent, D	−5.52 ± 2.57	−6.50 ± 2.13	0.003
Binocular mean intraocular pressure, mm Hg	15.82 ± 2.61	15.15 ± 2.41	0.064
Binocular mean lens thickness, mm	3.37 ± 0.16	3.33 ± 0.16	0.076
Binocular mean axial length, mm	25.65 ± 1.25	26.18 ± 1.24	0.003
Binocular mean BCVA (logMAR)	−0.01 ± 0.02	−0.01 ± 0.03	0.318

PBP, persistent Bergmeister's papilla; BCVA, best corrected visual ability; logMAR, logarithm of the minimum angle of resolution.

Table 3. Variance Analysis of the Three Forms of PBPs

Eyes	Type I 173 (66.8%)	Type II 59 (22.8%)	Type III 27 (10.4%)	F	*P* Value	$P_{I\text{-}II}$ /	$P_{I\text{-}III}$ /	$P_{II\text{-}III}$ /
Age, y	11.57 ± 2.77	12.41 ± 2.31	12.41 ± 2.45	2.873	0.058†	0.037	0.127	0.999
Height, m	1.51 ± 0.16	1.59 ± 0.14	1.58 ± 0.13	6.955	0.001†	0.001	0.043	0.668
Length/base width	1.96 ± 1.34	1.60 ± 0.67	0.70 ± 0.17	62.90	<0.001‡	0.178	0.000	0.000
Axial length, mm	25.27 ± 1.36	26.05 ± 1.10	26.14 ± 1.01	23.12	<0.001‡	0.000	0.005	1.000
Spherical equivalent, D	−4.82 ± 2.72	−6.24 ± 2.56	−6.56 ± 2.27	17.21	<0.001‡	0.003	0.005	1.000
Lens thickness, mm	3.35 ± 0.18	3.41 ± 0.13	3.40 ± 0.16	4.00	0.020‡	0.054	0.310	1.000
Intraocular pressure, mm Hg	15.89 ± 2.83	15.27 ± 2.69	16.46 ± 2.97	1.88	0.155†	/	/	/
BCVA (logMAR)	−0.01 ± 0.02	−0.01 ± 0.02	0.00 ± 0.02	0.19	0.827†	/	/	/

PBP, persistent Bergmeister's papilla; BCVA, best corrected visual ability; logMAR, logarithm of the minimum angle of resolution; *P*†,one-way ANOVA test (LSD test); *P*‡, Kruskal–Wallis test (Bonferroni correction).

Table 4. Stepwise Linear Regression Analysis of Predictors for Axial Length

	B	B	*P* Value
Height (m)	4.497	0.518	<0.001
PBP existence or not	−1.434	−0.54	0.041
Types of PBP	0.566	0.372	0.001

$R^2 = 0.349$, PBP, persistent Bergmeister's papilla; B, regression coefficient; β, Standardized regression coefficient.

PBP; in contrast, lower AL or degree of myopia corresponded to a greater incidence of type I PBP. There was a significant difference in LT between the three groups ($P = 0.024$); however, after post hoc tests, there was no significant difference among the three groups. There were no significant differences in BCVA and IOP among eyes with the three types of PBPs.

The PBP base was located more frequently in the nasal (187 eyes, 72.20%) than the inferior (58 eyes, 22.39%), temporal (12 eyes, 4.63%), and superior

Table 5. The Distribution of Three Forms of PBP in Different Axial Length Ranges

Axial Length (mm)	A ≤ 24	24 < A ≤ 25	25 < A ≤ 26	26 < A ≤ 27	27 < A
Eye, *n*	37	50	66	73	33
Type I, *n* (%)	34 (91.89)	38 (76.00)	43 (65.15)	43 (58.90)	15 (45.45)
Type II, *n* (%)	3 (8.11)	9 (18.00)	14 (21.21)	21 (28.77)	12 (36.36)
Type III, *n* (%)	0 (0)	3 (6.00)	9 (13.64)	9 (12.33)	6 (18.18)

(2 eyes, 0.77%) quadrants of the optic disc. In 25 eyes (25/259, 9.65%), a small stalk of fibrous tissue arising from the optic disc (grayish-white, thick, opaque masses were observed) was observed at the corresponding position on fundus photography.

Table 4 summarized the relationships among PBP existence or not, types of PBP, length/base width, sex, age, height, weight, BMI, IOP, LT, and BCVA (logMAR) with AL in stepwise linear regression models. The result shows that height, PBP existence or not, and types of PBP were independently associated with AL ($P < 0.001$, $P = 0.041$, and $P = 0.001$). Every 0.01 m increase in height was associated with a 0.045 mm increase in AL. Eyes with less PBP were likely to have a higher AL. Moreover, the morphology of PBP tended to be type III, even disappeared, were likely to have a higher AL.

Table 5 shows the distribution of three forms of PBP in different AL ranges. It shows that the proportion of PBP eyes in type I decreases gradually with AL, whereas in type II and type III, the proportion of PBP increases gradually with AL.

Discussion

After searching the PubMed database for papers published to May 1, 2019, using the keyword: "Bergmeister's papilla," we believe that our study is possibly the first to focus on the prevalence, morphology, and risk factors of PBPs in childhood. In this study, the prevalence of PBPs in children's eyes (67.80%) was much higher than that reported in previous studies using ophthalmoscopy (3%), fundus photography (0.03%), and autopsy (32.14%).[2–4] The prevalence reported herein is also higher than the results reported by Liu et al., who also used SS-OCT to observe 22 adults (50%).[5] We believe that this is due to the relatively young age of the participants in this study, which may partly support our previous hypothesis that PBP is gradually absorbed with growth and development in term-born children. Interestingly, we analyzed the clinical differences between the two groups of children with and without PBP and found that the height of children without PBP was significantly higher than that of children with PBP. In comparison, there was no significant difference in age between the two groups. These may be related to the fact that the subjects included in this study are children at the stage of rapid growth and development. The previous studies reported that height is the most effective indicator of children's growth and development and is more effective than age and weight.[8,9] Therefore, this may suggest that the absorption of PBP is accelerated in children with rapid growth.

However, eyeball development is not synchronized with the growth and development of individuals, which are affected by additional factors, such as educational exposure.[10] The growth of the eyeball is accompanied by refractive development. Children are born with mean hyperopic refraction and gradually turn to emmetropia.[11] Spillmann et al.[12] reported that myopia could begin at 4 to 6 years old and later, mainly due to the rapid growth of the eyes. In addition, Hung et al.[13] believed that in the process of emmetropization, abnormally excessive eye growth is one of the factors leading to myopia. The reflective development involves loss of corneal power, loss of lens power, and axial elongation. Cornea power stabilizes at the age of 5 to 6 years. Up to 10 to 12 years, there are rapid decreases in lens thickness and power and then slowly decreases. Whereas axial elongation can continue for as much as 20 years, rates seem to be influenced by the environments in which the children are growing up.[14] Our result also confirmed that there was a positive correlation between height and AL. Therefore, AL is one of the crucial indicators to reflect the development of eyeball and refraction.[15] Our study showed that, in myopic children, the group without PBP had significantly longer AL and more severe myopia than the group with PBP. Through logistic regression analysis, we confirmed that PBP existence or not was independently associated with AL. Therefore, we speculate that axial growth (growing myopia) may accelerate PBP absorption in myopic children. Similarly, we assume that the absence of PBP may reflect the faster axial growth, which needs to be conducted in a longitudinal cohort study to verify it in the future.

A previous study showed that the filaments gradually shortened until only a minute dot on the disc was visible, and this duly disappeared in followed up premature babies.[2] PBP is the colloid tissue and glial sheath of the hyaloid artery attached to the optic disc after incomplete atrophy of the hyaloid artery. We speculate that absorption of the PBP is similar to that observed in other organs, in which loose tissue (loose connective tissue surrounding the primary hyaloid artery) is the first to be absorbed and is followed by dense tissue connected to optic disc (primary hyaloid artery). Therefore, PBPs were divided into three categories according to the morphology of the body and base of the PBP on OCT images. We believe that the hyaloid arteries of the primary vitreous are often surrounded by some connective tissue in the early stage. On OCT images, the body shows a flame shape with irregular boundaries, which represents surrounding loose connective tissue, defined as type I. Subsequently, these loose connective tissues are gradually absorbed, and, in type II PBP, the connective tissue is ultimately clean, leaving only the internal dense vascular component, which corresponds to the cylindrical shape on OCT. The internal dense vascular component is also gradually absorbed, and the body becomes shorter and appears as a hilly shape on OCT images, which is denoted as type III PBP.

Our results show that in all eyes with PBP in myopic children, with the increase of AL (the degree of myopia increases), the main form of PBP gradually changes from type I to type II, and finally to type III. Moreover, types of PBP were independently associated with AL. These confirm our hypothesis that axial growth (growing myopia) may accelerate PBP absorption in myopic children. During the absorption process, PBPs may show great variety in their appearance, representing different stages. Therefore, they may also reflect the degree of myopia to some extent. In other words, the regression, even absence of PBP may reflect the faster axial growth (growing myopia), which needs to be verified by longitudinal cohort studies.

Most cases of PBP showed attachment to the nasal (72.2%) and inferior (22.39%) quadrants of the optic disc, and they were rarely distributed in the temporal (4.63%) and superior (0.77%) quadrants, which was consistent with the results observed by Roth et al. in autopsied eyes (74.5% in the nasal quadrant, and 24.2% in the nasal inferior quadrants).[3] This may be closely associated with the major vessels as the hyaloid artery merges.[3]

The limitations of this study are as follows. First, this study only observed Chinese myopic children, so it is impossible to speculate whether there are racial differences. Second, this was a cross-sectional study with a narrow age range (4–18 years), which cannot fully represent the evolution and absorption process of residues. This study was performed using the 12-line radial scanning mode for the optic disc, which may not fully describe the entire morphology of the residues and lead to omissions. Finally, the subjects of this study were myopic patients, which could not reflect the change of PBP under different refractive states. To further confirm our hypothesis, we will conduct a cohort study of current myopic children with long-term follow-up.

In conclusion, the prevalence and morphology of PBPs are closely related to AL. The findings suggest that PBPs may be a new indicator to judge the development of the myopia. A child's preoptic disc residue has converted to type III earlier or has been completely absorbed and disappeared may be more likely to have growing myopia and need more aggressive preventive treatment as early as possible. In the follow-up assessments, we will pay more attention to these children with an increased risk of developing high myopia.

Acknowledgments

Funded by the Chinese National Nature Science Foundation (Project Nos. 81670898 and 81600778).

Disclosure: **Q. Lin**, None; **J. Deng**, None; **K. Ohno-Matsui**, None; **X. He**, None; **X. Xu**, None

[*] QL and JD contributed equally to this study.

References

1. Bedell AJ, Jokl A. Epipapillary tissues. *Trans Am Ophthalmol Soc*. 1954;52:291–304.
2. Jones HE. Hyaloid remnants in the eyes of premature babies. *Br J Ophthalmol*. 1963;47:39–44.
3. Roth AM, Foos RY. Surface structure of the optic nerve head. 1. Epipapillary membranes. *Am J Ophthalmol*. 1972;74(5):977–985.
4. Bassi ST, George R, Sen S, Asokan R, Lingam V. Prevalence of the optic disc anomalies in the adult South Indian population. *Br J Ophthalmol*. 2019;103(1):94–98.
5. Liu JJ, Witkin AJ, Adhi M, et al. Enhanced vitreous imaging in healthy eyes using swept source optical coherence tomography. *PLoS One*. 2014;9(7):e102950.

6. Morgan IG, French AN, Ashby RS, et al. The epidemics of myopia: Aetiology and prevention. *Prog Retin Eye Res*. 2018;62:134–149.
7. Baird PN, Saw SM, Lanca C, et al. Myopia. *Nat Rev Dis Primers*. 2020;6(1):99.
8. Kulaga Z, et al. The height-, weight-, and BMI-for-age of Polish school-aged children and adolescents relative to international and local growth references. *BMC Public Health*. 2010;10:109.
9. Zheng W, Suzuki K, Yokomichi H, Sato M, Yamagata Z. Multilevel longitudinal analysis of sex differences in height gain and growth rate changes in Japanese school-aged children. *J Epidemiol*. 2013;23(4):275–279.
10. Hepsen IF, Evereklioglu C, Bayramlar H. The effect of reading and near-work on the development of myopia in emmetropic boys: a prospective, controlled, three-year follow-up study. *Vision Res*. 2001;41(19):2511–2520.
11. Cook RC, Glasscock RE. Refractive and ocular findings in the newborn. *Am J Ophthalmol*. 1951;34(10):1407–1413.
12. Spillmann L. Stopping the rise of myopia in Asia. *Graefes Arch Clin Exp Ophthalmol*. 2020;258(5):943–959.
13. Hung GK, Mahadas K, Mohammad F. Eye growth and myopia development: Unifying theory and Matlab model. *Comput Biol Med*. 2016;70:106–118.
14. Morgan IG, Rose KA, Ashby RS, Spaide RF, Ohno-Matsui K, Yannuzzi LA (eds). Pathologic Myopia, in: *Animal models of experimental myopia: Limitations and synergies with studies on human myopia*. New York, NY: Springer Science + Business Media; 2014:39–59.
15. Munro RJ, Fulton AB, Chui TY, et al. Eye growth in term- and preterm-born eyes modeled from magnetic resonance images. *Invest Ophthalmol Vis Sci*. 2015;56(5):3121–3131.